Research Square

Preprints are preliminary reports that have not undergone peer review.
They should not be considered conclusive, used to inform clinical practice,
or referenced by the media as validated information.

Generalizing the LoD Transition Space for Continuous Multi-Scale Representation using Straight Skeletons

Amin Gholami

amin.gholami@upwr.edu.pl

Wrocław University of Environmental and Life Sciences

Pawel Boguslawski

Wrocław University of Environmental and Life Sciences

Martijn Meijers

Delft University of Technology

Article

Keywords: LoD Transition Space, vario-scale representation, map generalization, straight skeleton, continuous level of detail, topological consistency

Posted Date: August 31st, 2026

DOI: https://doi.org/10.21203/rs.3.rs-10720298/v1

License: This work is licensed under a Creative Commons Attribution 4.0 International License.
Read Full License

Additional Declarations: No competing interests reported.

Generalizing the LoD Transition Space for Continuous Multi-Scale Representation using Straight Skeletons

Amin Gholami1, *, Pawel Boguslawski[1], and Martijn Meijers[2]

Amin Gholami: https://orcid.org/0000-0002-2792-4962

Pawel Boguslawski: https://orcid.org/0000-0002-1914-9214

Martijn Meijers: https://orcid.org/0000-0003-0923-5423

[1]Institute of Geodesy and Geoinformatics-Wroclaw University of Environmental and Life Sciences-Wroclaw-Poland

[2]GIS Technology-Faculty of Architecture and the Built Environment-Delft University of Technology-Delft-The Netherlands

Corresponding Author:

Amin Gholami

Email: amin.gholami@upwr.edu.pl

Author Emails:

Pawel Boguslawski: pawel.boguslawski@upwr.edu.pl

Martijn Meijers: b.m.meijers@tudelft.nl

Abstract:

Continuous multi-scale representation enables geographic features to evolve smoothly across Levels of Detail, avoiding abrupt transitions between independently generalized datasets. However, existing approaches provide limited support for complex transformations involving different geometric and topological configurations. This study generalizes the LoD Transition Space framework to represent continuous transformations between polygons, polylines, and points. The proposed approach uses straight-skeleton-based geometric primitives to construct continuous 2D+1D transition volumes and decomposes complex transformations into localized LoD Transition Regions. The framework supports polygon-to-boundary-polyline, polyline-to-polyline, polygon-to-polygon, and N-to-M polygon transformations, including aggregation, merging, splitting, simplification, and collapsing. Horizontal slicing of the resulting 3D model generates intermediate representations at arbitrary Levels of Detail while maintaining geometric continuity and topological consistency. The approach was evaluated using real-world datasets from OpenStreetMap, NUTS, ATKIS, and Polish administrative and BDOT10k data. The experiments demonstrate that the framework can represent both regular and irregular multi-scale transformations, including cases where source and target geometries have complex spatial relationships or identical target extents. The proposed 3D model provides a unified representation for continuous map generalization and supports the generation of consistent intermediate representations across scales.

Keywords: LoD Transition Space; vario-scale representation; map generalization; straight skeleton; continuous level of detail; topological consistency.

1. Introduction

The increasing use of web-based Geographic Information Systems (GIS) and interactive mapping requires geographic data to be represented continuously across scales. However, most systems still rely on discrete Levels of Detail (LoDs), where independently generalized datasets are selected at predefined scales. This can cause abrupt changes during zooming, as features suddenly appear, disappear, merge, or change shape. Discrete LoDs also introduce data redundancy and make it difficult to maintain consistent spatial relationships across scales (Van Oosterom, 2005; van Oosterom and Meijers, 2011, 2014). Vario-scale representation addresses these limitations by treating scale as a continuous dimension, allowing representations at arbitrary scales to be derived from a unified model (Ai, 2010; van Oosterom and Meijers, 2014).

The Space-Scale Cube (SSC) provides a framework for representing geographic features together with scale as a 2D+1D structure, where the third dimension represents the evolution of features across scales (Meijers and van Oosterom, 2011; van Oosterom et al., 2014). The Dual Half-Edge (DHE) provides a complementary topological structure for representing and navigating the integrated geometry (Boguslawski and Gold, 2016). Nevertheless, a general geometric framework for constructing continuous transitions between different feature types and complex generalization operations remains limited.

Previous works established a straight-skeleton-based LTS approach for polygon-to-point and polygon-to-polyline transitions and integrated it with the DHE and SSC frameworks (Gholami et al., 2025, 2026). However, more complex transformations, including polygon-to-polygon, polygon-to-boundary-polyline, polyline-to-polyline, and N-to-M polygon transitions, require additional geometric and topological mechanisms. These transformations are important for map generalization operations such as merging, aggregation, simplification, splitting, collapsing, and smoothing.

This study generalizes the LoD Transition Space (LTS) framework to support these complex transformations. The proposed method represents LoD evolution as an additional dimension and constructs continuous 2D+1D transition volumes using straight-skeleton-based geometric primitives. Complex transformations are decomposed into localized LoD Transition Regions and integrated into a unified transition space. Horizontal slicing of this space enables the generation of arbitrary intermediate LoDs while maintaining geometric continuity and topological consistency.

The main contributions are: (1) a generalized LTS framework supporting diverse geometric and topological transformations; (2) a volumetric construction strategy for complex map generalization operations; and (3) a straight-skeleton-based reflection and extrusion method for polygon-to-boundary-polyline transitions. The proposed framework is demonstrated using synthetic and real-world datasets to evaluate its ability to generate continuous intermediate representations across scales.

2. Related Work

Research relevant to continuous LoD representation can be grouped into three areas: continuous geometric transformations, vario-scale map generalization, and topological consistency.

2.1. Continuous geometric transformations

The geometric basis of continuous feature transformation originates from the lifespan model, which describes the validity of geographic features across scale (Ai and Li, 2009), and from the straight skeleton and roof model. A straight skeleton is generated through inward wavefront propagation, where edge and split events describe progressive geometric changes (Aichholzer et al., 1996; Huber, 2011). Extensions of straight-skeleton methods have addressed irregular polygon configurations (Li et al., 2018; Li et al., 2019), while skeleton-based approaches have also been used for polygon-to-polyline transformations (Haunert and Sester, 2008; Li et al., 2022; Ren et al., 2021; Biedl et al., 2015).

Dimension-changing transformations between polygons, polylines, and points have been studied for feature collapse, aggregation, and geometric interpolation. Polygon-to-point transformations have been investigated by Wolf (2009), Choi and Hwang (2009), Gedicke et al. (2021), and Kronenfeld et al. (2020), while polygon-to-polygon and polyline-to-polyline transformations have been addressed using interpolation and morphing approaches (Barequet et al., 2003; Barequet and Vaxman, 2007; Kels and Dyn, 2011; Forsch et al., 2024; Dalstein et al., 2015). Related approaches have also reconstructed 3D objects from 2D contours using interpolation and straight-skeleton techniques (Oliva et al., 1996; Turk and O'Brien, 2005), and topology-preserving representations have emphasized the validity of intermediate geometries (Zeng et al., 2021). Road-network studies similarly demonstrate the importance of stable structural elements during continuous transformations (Strano et al., 2012).

Gholami et al. (2025) integrated the Straight Skeleton, Dual Half-Edge (DHE), and Space-Scale Cube (SSC) to support polygon-to-point and polygon-to-polyline transitions. However, the approach mainly addressed individual polygon collapse and did not provide a unified solution for neighboring features and more complex multi-feature transformations. DHE provides an appropriate topological foundation for such extensions because it supports representation and navigation of complex 3D geometries (Boguslawski, 2011; Boguslawski and Gold, 2016). Table 1 summarizes representative studies according to their primary dimension-changing transformations.

Table 1. Cited works are grouped by their primary dimension-changing transformation.

Object transformation	References
Polygon-to-point	(Gholami et al., 2025), (Wolf, 2009), (Choi and Hwang, 2009) , (Gedicke et al., 2021) and (Kronenfeld et al., 2020).
Polygon-to-polyline	(Gholami et al., 2025), (Aichholzer et al., 1996), (Haunert and Sester, 2008), (Li et al., 2022), (Gedicke et al., 2021), (Biedl et al., 2015), (Ren et al., 2021), (Haunert and Sester, 2008).
Polygons-to-polygons	(Gedicke et al., 2021), (Sarmah et al., 2023) , (Barequet et al., 2003), (Forsch et al., 2024), (Dalstein et al., 2015), (Barequet and Vaxman, 2007), and (Kels and Dyn, 2011).
Polyline-to-polyline	(Forsch et al., 2024) , (Dalstein et al., 2015), and (Zhang et al., 2024).

2.2. Map generalization and vario-scale representation

Map generalization transforms detailed geographic data into smaller-scale representations through operations such as simplification, aggregation, displacement, typification, and elimination. Conventional approaches generally produce discrete LoDs, whereas vario-scale representation treats scale as a continuous dimension and enables smooth transitions between representations (Ai, 2010; van Oosterom and Meijers, 2014).

The Space-Scale Cube (SSC) provides a fundamental framework for this concept by representing 2D geographic features together with scale as a 2D+1D volumetric structure

(Meijers and van Oosterom, 2011; van Oosterom et al., 2014). The vertical extent represents the lifespan of features across scale, while topological data structures such as the DHE support integrated geometric and relational information (Karim et al., 2017). Previous work has demonstrated the application of such structures to multi-scale data management (Gholami et al., 2024). Other approaches have explored graph-based aggregation (Rottmann et al., 2021; Rottmann et al., 2025), triangulation-based methods (Jones et al., 1995), continuous road-network generalization (Šuba et al., 2016), vector pyramids (Yang et al., 2021), matrix-based representations (Huang et al., 2017), and Fourier-based continuous models (Liu et al., 2016). GHS-SmartDissolve provides an effective approach for producing dissolved polygon layers but does not explicitly represent the intermediate transition states (Schiavina et al., 2023). Similarly, generic representations for heterogeneous point, line, and polygon datasets have been proposed without incorporating a continuous scale dimension (Rolland et al., 2024).

Continuous LoD transitions have also been investigated for 3D building models (Kada et al., 2015; Yang et al., 2024). However, existing approaches generally focus on particular object types or mesh-based transformations and do not provide a unified framework for simultaneous map generalization operations involving different geometry types.

Recent work by (Gholami et al., in press) addressed the topological integration of separate multi-scale datasets using a primal–dual data structure, producing a unified 3D vario-scale representation and reducing geometric redundancy through deep integration. However, that framework primarily establishes structural relationships among existing representations rather than explicitly modeling the continuous geometric evolution between them. The present study complements this approach by introducing an LTS-based framework for constructing and slicing the transition between source and target representations.

2.3. Topological consistency

Preserving topology during map generalization is essential for avoiding invalid spatial relationships. Topology-preserving simplification has been investigated by Saalfeld (1999) and Visvalingam and Whyatt (2017), while the 9-intersection model has been extended to represent spatial relationships under different levels of resolution and abstraction (Tinghua and Yaolin, 2003). Gorshkov et al. (2022) compared the 9IM, topological chain, and E-WID models, while Cheng et al. (2023) introduced concept-neighborhood graphs for evaluating topological similarity during dimension-changing transformations. Torres-Avilés et al. (2025) further

proposed an efficient representation for computing DE-9IM relationships over large polygon datasets.

Despite these developments, existing approaches generally evaluate or preserve topology at discrete states rather than explicitly modeling its continuous evolution during LoD transitions. Similarly, existing geometric interpolation methods do not directly integrate continuous transformation with a topology-aware vario-scale representation.

Therefore, a gap remains between continuous geometric transformation, vario-scale representation, and topology-preserving map generalization. The present study addresses this gap by extending the LoD Transition Space (LTS) framework of Gholami et al. (2026) to polygon-to-boundary-polyline, polygon-to-polygon, polyline-to-polyline, and N-to-M polygon transformations. The proposed approach represents these transformations as continuous 2D+1D volumes that can be sliced at arbitrary LoDs, providing a unified framework for generating intermediate representations while maintaining geometric continuity and topological consistency.

3. Method and Materials for the LTS for other cases

This section extends the LTS by detailing the LTS construction for diverse geographic feature types, such as lines and complex polygon networks, beyond the initial polygon-to-point case.

3.1 Polygon-to-boundary-polyline transition

The purpose of this section is to describe the polygon-to-boundary-polyline transition transitions a polygon to a subset of its boundary edges.

As shown in Fig. 1, given a polygon P (source at $l = 0$) and a subset S (target at $l = 1$) as inputs, the proposed approach generates the 3D representation of the LoD transition space between these source and target geometries in four steps.

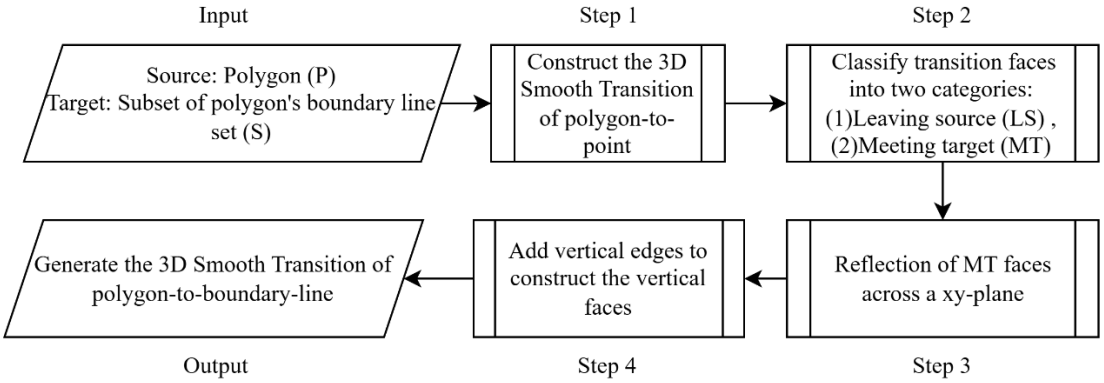


Fig. 1. The flowchart of steps to generate the polygon-to-boundary-polyline transition.

The proposed approach consists of four steps.

Step 1. Construct the LTS using the straight skeleton over the l-range such that the highest point has $l = 0.5$. Thus, $H_p = (x, y, 0.5)$, and the horizontal plane passing through this point is defined by $l = 0.5$, denoted as the H_p plane.

Step 2. Classify the transition faces into two categories: Leaving Source (LS) faces and Meeting Target (MT) faces. An LS face corresponds to a transition face (e_i) where $e_i \in S$, and an MT face corresponds to a transition face (e_i) where $e_i \notin S$.

Step 3. Reflect the MT faces across the H_p plane. The reflection transformation of a vertex with coordinates (x, y, l) across the H_p plane yields $(x, y, 1 - l)$; thus, transform each vertex of the MT faces individually.

Step 4. Add extrusion edges between the reflected MT faces, the LS faces, and the source faces to construct the extrusion faces. This step extends the LTS lifespan to the full l-range.

This methodology ensures a continuous and smooth transformation between the source polygon and the target boundary subset, facilitating the generation of intermediate levels of detail.

For illustration, consider the polygon P as the source with $E = \{e_1, e_2, \dots, e_9\}$, and one subset of E as the target, for instance $BE = \{e_5, e_6, e_7, e_8, e_9\}$.

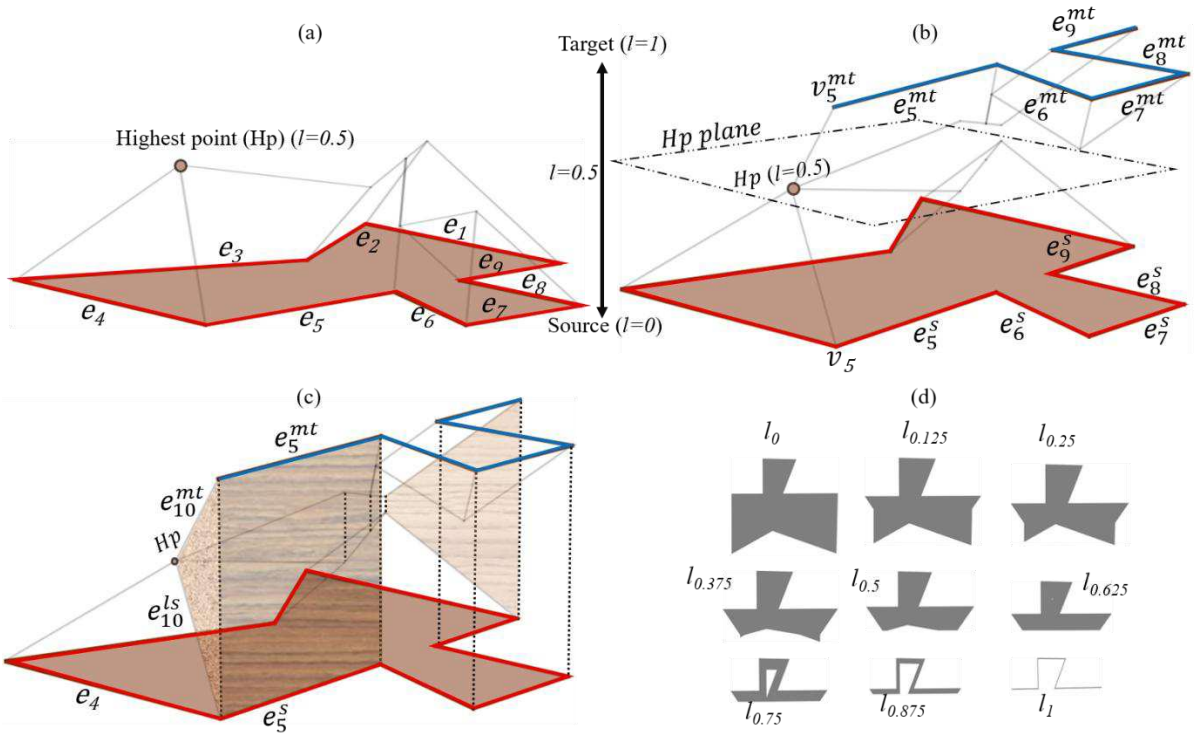


Fig. 2. Generating the polygon-to-boundary-polyline transition; (a) construct the 3D smooth transition of polygon-to-point (step 1). (b) reflection of MT faces across a horizontal plane (step 3). (c) construct the extrusion faces (step 4) then the final polygon-to-boundary-polyline transition is constructed. (d) slicing illustration in 9 horizontal planes.

In summary, the polygon-to-boundary-polyline transition can be achieved by extruding the polygon-to-point transition along the MT faces, as this preserves the straight skeleton's planar transition faces while extending the structure to the full *l-range*, ensuring a continuous and watertight solid volume.

Due to the reflection across the H_p plane ($l = 0.5$), each vertex $v_i = (x_i, y_i, l_i)$ in an MT face (where $l_i \neq 0.5$) maps to a new vertex at $v_i^{mt} = (x_i, y_i, 1 - l_i)$, as illustrated by v_5 and v_5^{mt} in Fig. 2b. This symmetric reflection maintains geometric consistency and avoids discontinuities in the transition.

For each edge in the target subset S, extrusion faces are constructed by connecting its vertices to their reflected counterparts:

- If the edge (e.g., e_5) is horizontal and not on the H_p plane, the extrusion yields a rectangular face.
- If one vertex lies on the H_p plane, the face forms an isosceles triangle.

- If neither vertex is on the H_p plane and the edge is non-horizontal, the face is an isosceles trapezoid.

These extrusion faces, combined with the LS and reflected MT faces, complete the polygon-to-boundary-polyline transition, forming a solid volume whose horizontal slices at any $l \in$ yield the intermediate polygon geometry (Fig. 2d illustrates nine slices animating the LoD transition from polygon-to-boundary-polyline).

This construction guarantees smooth, topologically valid LoD transitions: slicing from $l = 0$ (full polygon P) to $l = 1$ (boundary line subset S) produces monotonic shrinkage without self-intersections, and vice versa.

The LTS for boundary-line-to-polygon is obtained by reversing l in the polygon-to-boundary-polyline transition via $l' = 1 - l$, thereby swapping the roles of source (boundary line subset at $l' = 0$) and target (polygon at $l' = 1$), as depicted in Fig. 3.

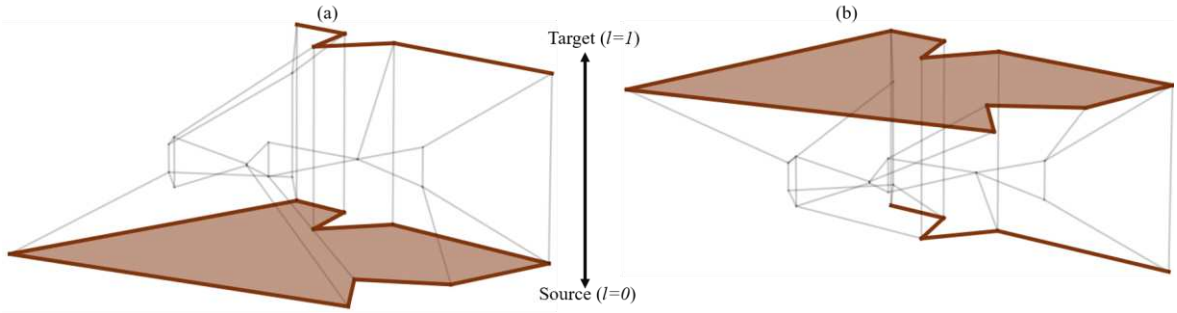


Fig. 3. Reversing the LTS; (a) polygon-to-boundary-polyline transition and (b) LTS for boundary-line-to-polygon.

3.2 Polygon-to-polyline transition

In polygon-to-polyline transition, the source polyline $S = \langle s_1, s_2, \dots, s_n \rangle$ at $l = 0$ transits to a target polyline $T = \langle t_1, t_2, \dots, t_n \rangle$ at $l = 1$. The construction of the LTS involves three main steps: project T onto the plane of S and identify the appropriate LoD transition regions based on their topological relationships; construct the LTS for each LTR; and remove certain extrusion and source edges, or in some cases, transition faces.

Step1. After projection of the polylines there are 57 possible topological relationships between two polylines (Egenhofer and Herring, 1990). If the polylines do not overlap, they define one or more areas between them, which serve as LTRs. These polylines may intersect at their endpoints (Fig. 4a), at non-endpoints (Fig. 4c), or not intersect at all (Fig. 4b). If

endpoints do not touch, bridge edges (dotted lines in Fig. 4b and 4c) connect them to enclose the LoD transition region. However, non-overlapping cases can be unsatisfactory for several reasons: in dangling edge cases, bridge edges may intersect the polylines, preventing an LTR that includes all segments; or the polylines may be weakly connected. Overlapping cases are also unsatisfactory, as no LTR exists.

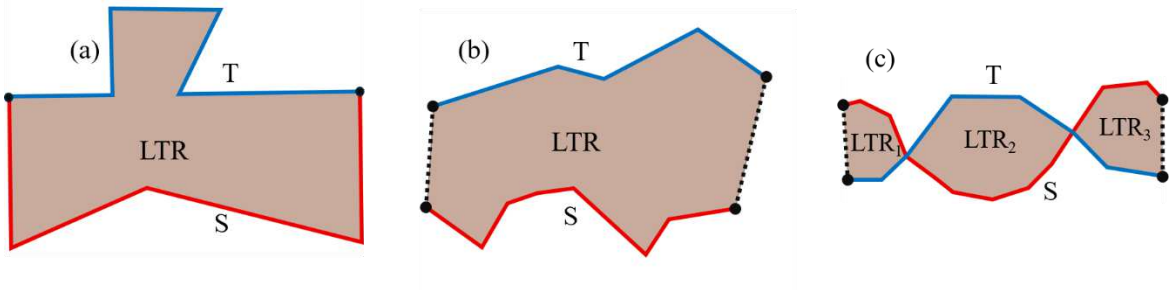


Fig. 4. The LoD transition region (LTR) for polyline-to-polyline is defined by two input polylines source and target whether with their (a) intersection, (b) along with their bridge edges (dotted lines), or (c) both.

Step2. With the LTR defined, Step 2 involves constructing the individual polygon-to-boundary-polyline transition solid volumes for each identified LTR. For each LTR, source and target edges, along with any applicable bridge edges, are identified. Bridge edges can be treated as either source or target edges; in this paper, they are considered source edges and removed later if necessary (see Fig. 6). In Fig. 5, the construction of the LTS for the polyline-to-polyline transition for the two polylines in Fig. 4a is illustrated. In this case, there are no bridge edges, so the polygon-to-boundary-polyline transition is constructed with the polygon P as the source ($E = \{e_1, e_2, \dots, e_9\}$) and one subset of E as the target ($BE = \{e_5, e_6, e_7, e_8, e_9\}$).

Step 3. The final step involves removing all target edges from the source polygon ($e_5^s, e_6^s, e_7^s, e_8^s, e_9^s$) and the extrusion edges of vertices belonging to two target edges ($e_{v6}^{ex}, e_{v7}^{ex}, e_{v8}^{ex}, e_{v9}^{ex}$). The remaining solid volumes form the LTS for the polyline-to-polyline transition.

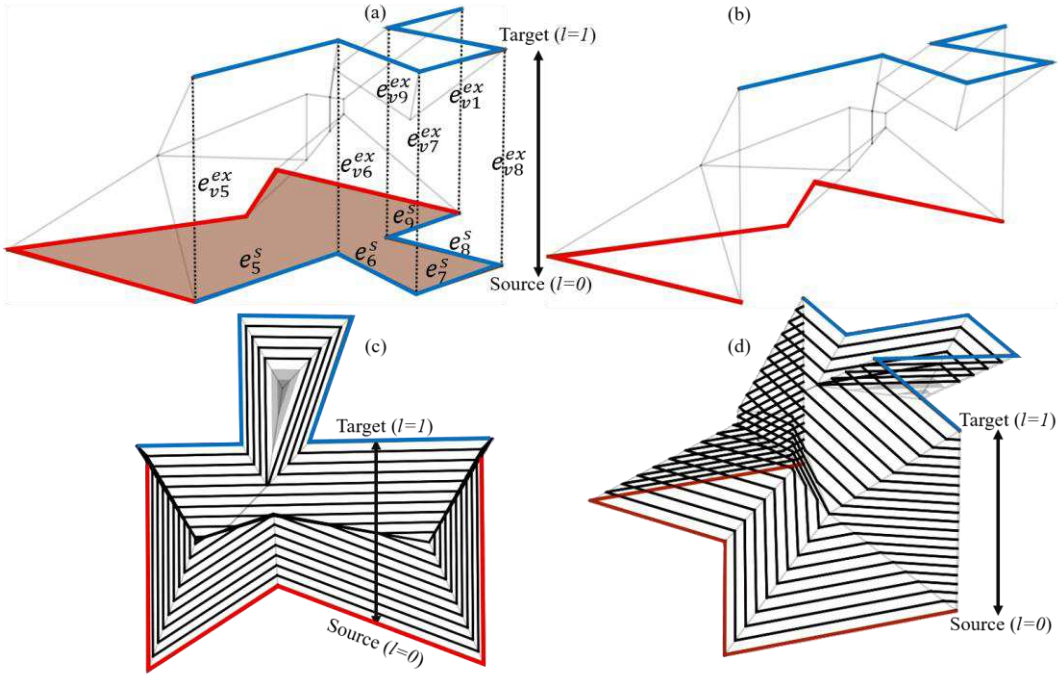


Fig. 5. LTS for polyline-to-polyline when endpoints touch: (a) construction of the polygon-to-boundary-polyline transition; (b) removal of some source and extrusion edges; and slicing illustrations from (c) top and (d) isometric views.

In Fig. 5c, d illustrates the slicing of the solid volumes, showcasing the generation of intermediate LoDs between the source and target polylines, which is crucial for achieving smooth transitions in vario-scale representations.

In the LTR containing a bridge edge, the decision of whether to remove its corresponding faces depends on whether these bridge edges contribute to the structural integrity or visual continuity of the intermediate LoDs. This determination can be guided by analyzing the impact of such removals on the overall geometric and topological coherence of the vario-scale representation. In Fig. 6a-d, the impact of removing the corresponding bridge faces is shown, along with their slicing illustrations.

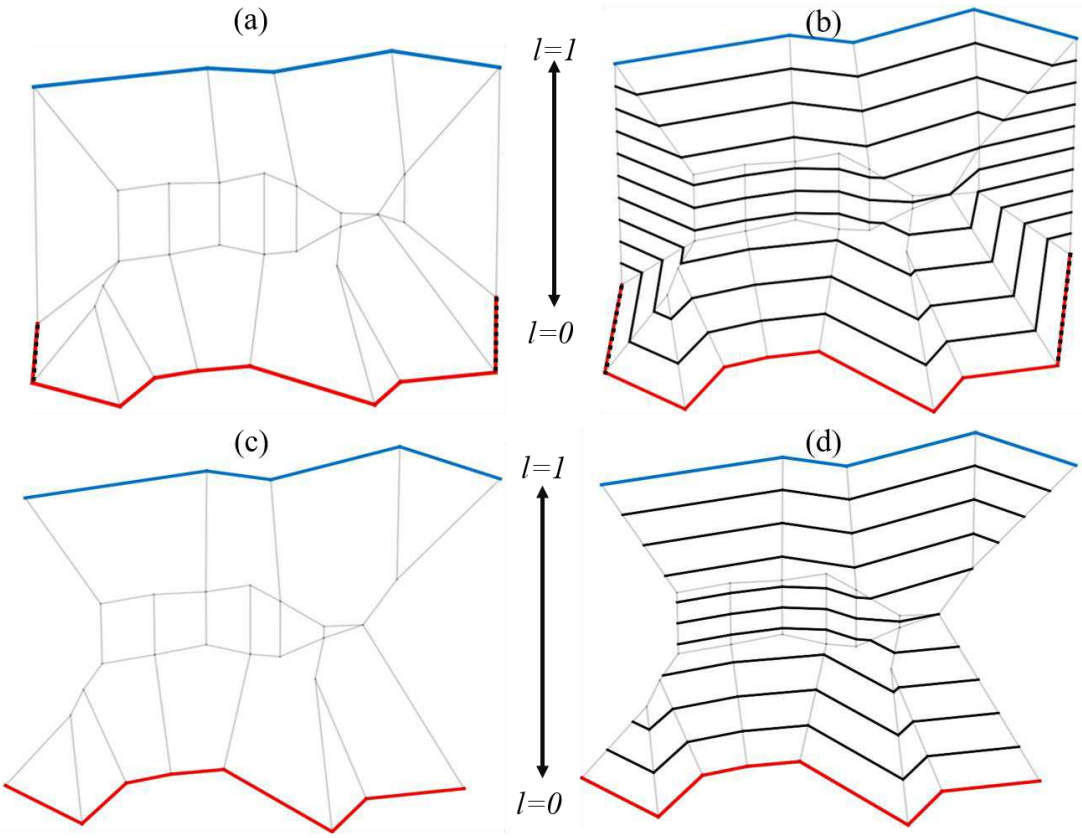


Fig. 6. LTS for polyline-to-polyline process when polylines do not intersect at all: (a) construction of the LTS including bridge edges and its (b) slicing illustration; (c) removal of the LS faces of bridge edges and their corresponding extrusion faces, and its (d) slicing illustration.

3.3 Polygon-to-polygon transition

In the polygon-to-polygon transition, the source polygon at $l = 0$, is denoted by S, and a target polygon at $l = 1$, is denoted by T. The proposed framework generates a unified 2D+1D solid representation that enables smooth and topologically consistent transitions between the two polygonal states through continuous slicing along the LoD dimension.

The proposed construction of the polygon-to-polygon transition space is divided into three main steps:

1. overlay and identification of active LoD Transition Regions,
2. construction of local LTS solid volumes within each active LTR, and
3. splicing of the generated LTS volumes into a single coherent transition space.

Step 1. Overlay and Identification of Active LTRs

In the first step, the target polygon T is projected onto the plane $l = 0$ (see Fig. 7a), such that both polygons S and T are represented in a common two-dimensional space. After overlay, the polygons may exhibit one of the six standard topological relationships defined in the DE-9IM model: disjoint, touch, overlap, contains/within, equals, and covers/coveredBy (Egenhofer and Herring, 1990).

At the current stage, the proposed polygon-to-polygon framework focuses on the satisfying cases in which the interiors of the polygons overlap, i.e., $S^\circ \cap T^\circ \neq \emptyset$ and $S \neq T$, which correspond to the overlap, contains/within, and covers/coveredBy relationships. The disjoint and touch relationships are considered non-satisfying cases in this work, since they require additional handling strategies to preserve spatial continuity and topological consistency during the transition process.

To determine the regions where geometric transformation actively occurs, the symmetric difference between the source and target polygons is computed: $S\Delta T = (S \cup T) - (S \cap T)$. The resulting regions define the active LTRs, whereas the intersection $S \cap T$ defines the inactive LTRs (see Fig. 7a). Consequently, smooth geometric evolution occurs only within regions where the source and target polygons differ, while unchanged regions remain geometrically stable throughout the transition.

For the subsequent construction of the polygon-to-polygon transition space, two alternative modeling strategies can be considered. In the first strategy, the transition is decomposed into a collection of localized transformations within the active LTRs. Depending on the geometric configuration of each region, the corresponding LTS solid volumes are generated using polyline-to-polyline, polygon-to-point, or point-to-polygon transitions. These local transition volumes are subsequently connected through their adjacent vertical edges to produce a continuous global LTS.

In the second strategy, the transition is modeled using polygon-to-boundary-polyline and boundary line to polygon transformations across both active and inactive LTRs. The resulting transition volumes are then integrated by merging their adjacent vertical faces.

In this paper, we adopt the first strategy, as it provides a more flexible and geometrically robust framework for modeling complex polygonal transformations while preserving local topological relationships throughout the LoD evolution.

Step 2. Construction of Local LTS Volumes

The second step involves constructing the LTS solid volumes for each active LTR according to its geometric characteristics.

If an active LTR contains both source and target boundary segments (e.g., LTR_1, LTR_2, LTR_3, andLTR_4 in Fig. 7a), the transition volume is constructed using the previously described polyline-to-polyline approach, where source edges at $l = 0$ gradually transform into target edges (see Fig. 7b).

If an active LTR contains only source edges e.g.LTR_5in Fig. 7a, the region represents a disappearing component of the source polygon. In this case, the transition is modeled using the polygon-to-point LTS, where the polygonal region continuously collapses into a point as $l \to 1$ (see Fig. 7).

Conversely, if an active LTR contains only target edges e.g.LTR_6in Fig. 7a, the region corresponds to a newly emerging component in the target polygon. Such regions are modeled using the Pt2P LTS, where a point at $l = 0$ progressively expands into the target polygonal geometry at $l = 1$ (see Fig. 7b).

In Fig. 7c, the slicing illustration before splicing is shown. Since the individual LTS volumes for the polyline-to-polyline transitions in each active LTR are not connected at their boundaries, they cannot form a closed shell. Consequently, the corresponding slicing geometry for each LTS for polyline-to-polyline appears as an open polyline. To resolve this, we perform a splicing operation that merges adjacent polyline-to-polyline volumes by their shared vertical edges, ensuring a watertight integration of the generated components.

Step 3. Splicing of Local LTS Volumes

The final step consists of spatially integrating the locally generated LTS solid volumes into a single continuous polygon-to-polygon transition space (see Fig. 7d). This integration is performed by splicing adjacent LTS volumes along their shared vertical edges, ensuring geometric continuity and topological coherence across neighboring transition regions.

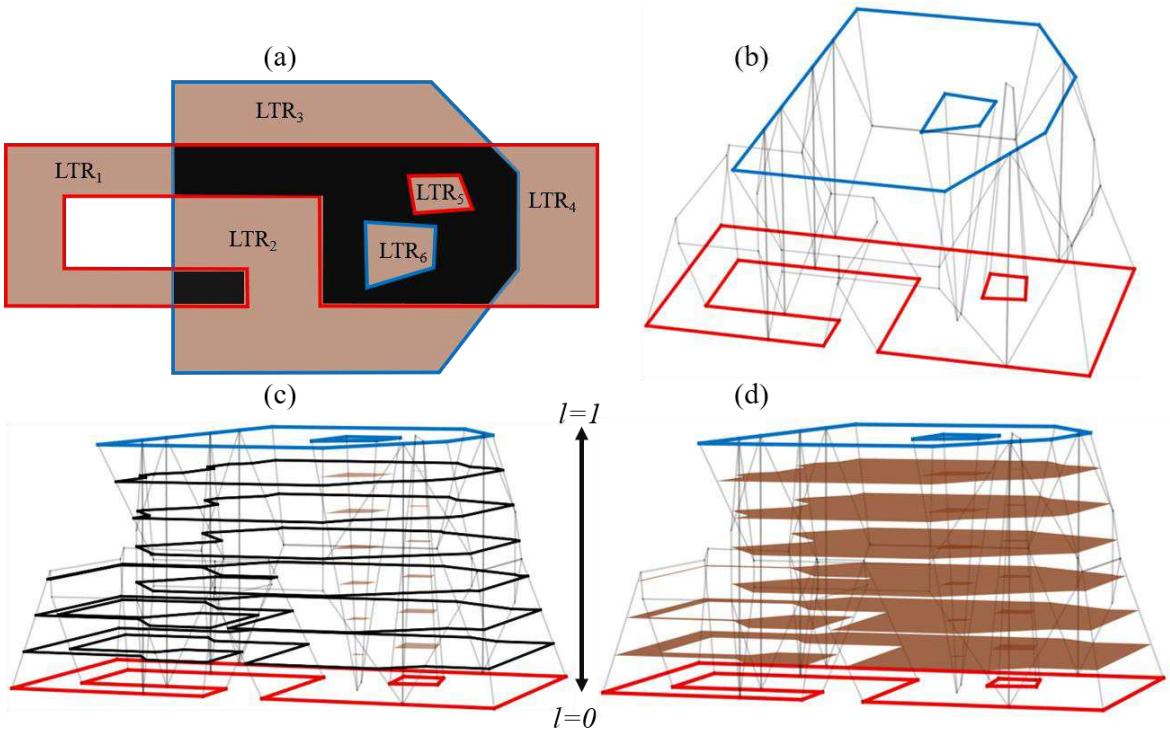


Fig. 7. Polygon-to-polygon transition process : (a) input source and target polygons with overlapping regions, including the identification of active LTRs (brown regions) and inactive LTRs (black regions), (b) independent construction of local LTS solid volumes for each active LTR together, illustrative horizontal slices, (c) before and (d) after splicing ; In the slicing visualizations, resulting polylines are represented by black solid lines, while polygonal regions are illustrated as filled brown polygons.

Furthermore, when the source and target polygons contain holes, whose interiors do not overlap, as illustrated in Fig. 7, two alternative strategies can be considered.

The first strategy treats each hole independently by allowing holes to appear or disappear individually during the LoD transition process. In this approach, disappearing holes are modeled using polygon-to-point transitions, while emerging holes are generated using Pt2P transitions.

The second strategy aims to transform corresponding holes smoothly and continuously by constructing the polygon-to-polygon transitions between the holes themselves. However, since non-overlapping holes correspond to disjoint topological relationships, they currently fall into the category of unsatisfying cases for which a robust transition model has not yet been introduced. Therefore, in the present work, we adopt the first strategy and handle holes through independent appearance and disappearance operations. For addressing the cases of disjoint or

touching polygons, future work will explore methods for creating intermediate geometries that bridge the gap or separate the touching boundaries.

The resulting global LTS forms a manifold 2D+1D structure that supports smooth interpolation between the source and target polygons while avoiding discontinuities and visual artifacts during the LoD transition process. This systematic assembly of localized transition volumes provides a robust framework for modeling complex polygonal transformations across continuous levels of detail. Furthermore, because the constructed LTS represents a continuous volumetric space, infinitely many intermediate polygonal states can be generated by slicing the transition space at arbitrary values of $l \in [0,1]$. This approach significantly advances existing multi-LOD representation techniques by enabling continuous geometric and topological transformations rather than relying on discrete state changes.

3.4 N-to-M-polygons transition

N-polygons-to-M-polygons is an extension of the polygon-to-polygon transition, where the complexities introduced by varying numbers of input and output geometries. This extension necessitates a sophisticated approach to establish correspondence mappings between disconnected components, especially when considering scenarios involving polygon splitting and merging events.

To address transitions from N source polygons to M target polygons, we first compute the union of all source polygons to form a single composite source geometry S, and analogously union all target polygons into a composite target T. This reduces the $N{:}M$ problem to an effective single polygon-to-polygon transformation, for which the LTS construction process (including LTR identification, local LTS volume generation, and splicing) proceeds identically as described in the previous section. The core challenge in such N-to-M-polygons transformations lies in defining a coherent and continuous morphing process that accurately reflects the geometric and topological evolution from source to target.

4. Applications in Vario-scale representation

The proposed LTS framework was evaluated using several real-world datasets representing different types of multi-scale geometric transformation. The experiments focus on polygonal aggregation, irregular multi-scale transitions, and hierarchical regional structures.

4.1. polygonal Aggregation

The first application considers the aggregation of detailed building footprints into a more generalized representation. A real-world dataset from Great Neck, New York, USA, was used to demonstrate the transition from multiple building polygons to an aggregated target region (Fig. 8a).

After projecting the target onto the source layer, the target contains the corresponding source features. Their symmetric difference therefore forms a polygon with multiple holes, with the outer boundary defined by target edges and the inner boundaries by source edges. The proposed LTS construction generates a continuous transition between these configurations while preserving their geometric and topological relationships (Fig. 8b). Horizontal slicing produces intermediate representations at arbitrary LoDs, demonstrating a gradual aggregation process rather than a discrete change between source and target geometries (Fig. 8c).

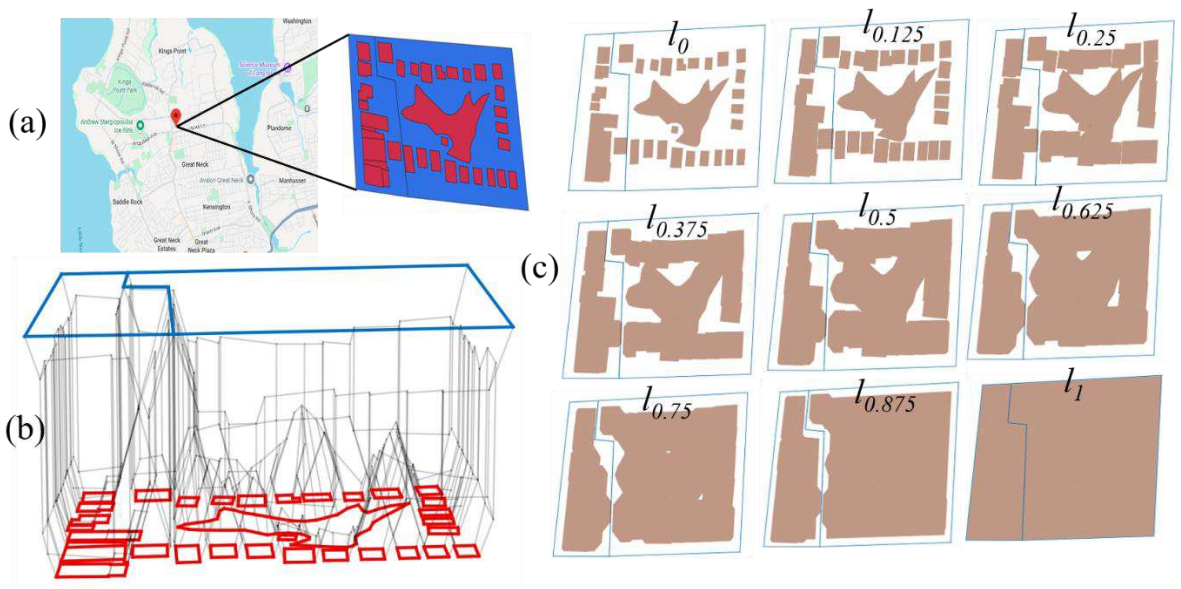


Fig. 8. polygonal aggregation using the proposed LTS framework: (a) first case study area in Great Neck, New York, USA; (b) constructed LTS representing the smooth aggregation process between polygonal features; (c) illustration of horizontal slicing from top view, demonstrating the generation of continuous intermediate geometries throughout the aggregation transition.

4.2. Irregular Geometry Transitions in Multi-scale Layers

Real-world multi-scale datasets often involve several generalization operations simultaneously rather than a single regular transformation. To evaluate this situation, the NUTS 2024 polygon dataset from the Eurostat GISCO database was used. A region of the South Aegean islands in Greece was selected because of its fragmented multipart geometry and complex coastal

boundaries (Fig. 9a). The 03M dataset was used as the source and the 10M dataset as the target (Fig. 9b).

The transition involves several operations simultaneously, including aggregation, splitting, merging, exaggeration, simplification, elimination, orientation, and displacement. For example, Fig. 9b1 shows simultaneous simplification and exaggeration, Fig. 9b2 illustrates aggregation followed by splitting, and Fig. 9c1 demonstrates merging followed by simplification. The resulting LTS provides a continuous transition between these heterogeneous configurations and maintains the overall topological structure throughout the transformation (Fig. 9c). Horizontal slicing generates intermediate representations across the LoD range (Fig. 9d).

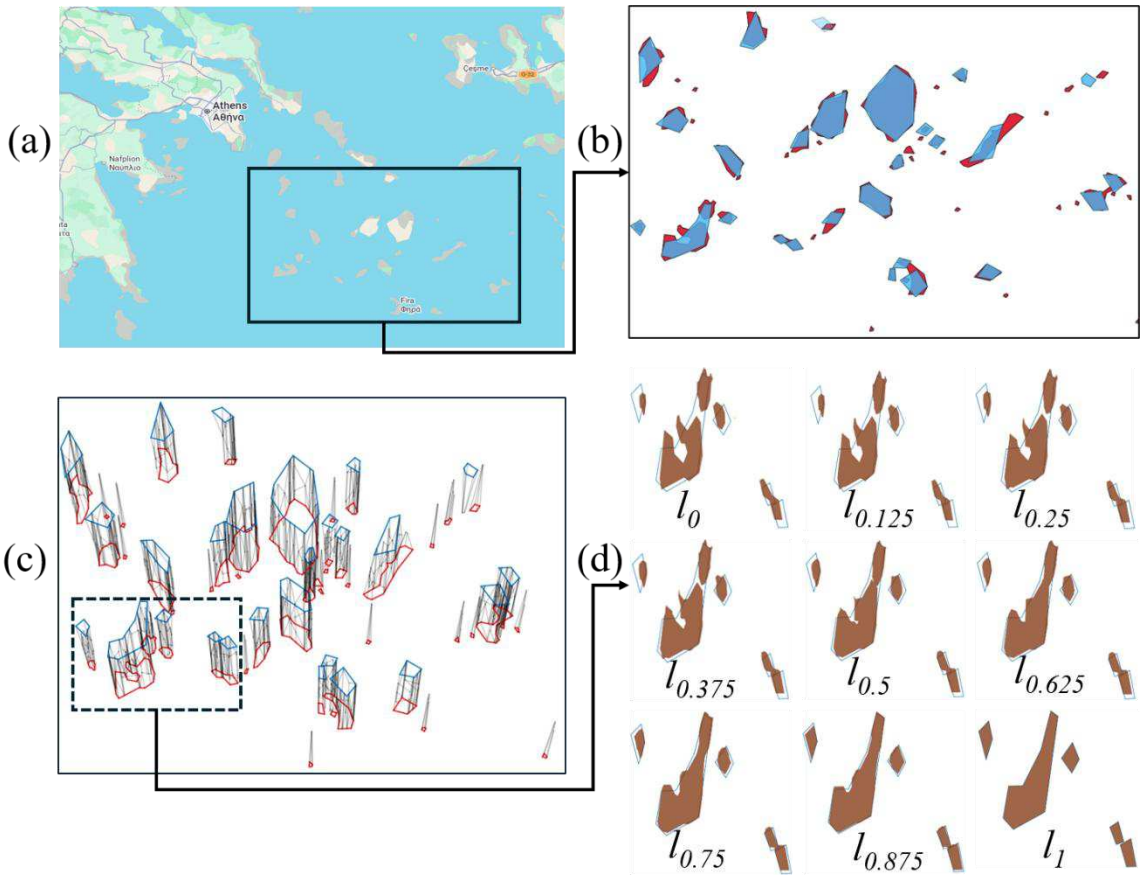


Fig. 9. Application of the proposed LTS framework to non-regular multi-scale polygonal structure;(a) case study area covering the South Aegean islands in Greece. (b) projection of the source and target polygonal layers ;(c) constructed LTS representing the continuous transition between the multi-scale polygonal layers; (d) top-view visualization of horizontal slicing.

Some transformations produce disjoint source and target regions after projection, for which symmetric difference may not provide a direct transition region. In these cases, the

framework uses the available geometric relationships to represent the appearance and disappearance of features through the transition process. Cases in which the symmetric difference is empty require specialized strategies, as demonstrated below.

4.3. Regional hierarchical structure

Hierarchical regional datasets provide a different challenge because a target region may completely contain the union of its source regions. In such cases, the symmetric difference is empty and cannot directly define active LTRs. Two strategies were therefore investigated.

The first strategy performs sequential merging of neighboring polygons using polygon-to-boundary-polyline transitions. The German ATKIS dataset, representing a rural area near Hamburg at a nominal scale of 1:50,000, was used for this experiment. The dataset contains 525 source polygons, which are progressively merged according to feature importance until a single generalized target region is obtained (Fig. 10a). An LTS is constructed for each consecutive merging step, and the resulting transition spaces are integrated into a unified LTS, where (l=0) represents the initial configuration and (l=1) the final configuration (Fig. 10b). Horizontal slicing provides the intermediate states of the merging process (Fig. 10c).

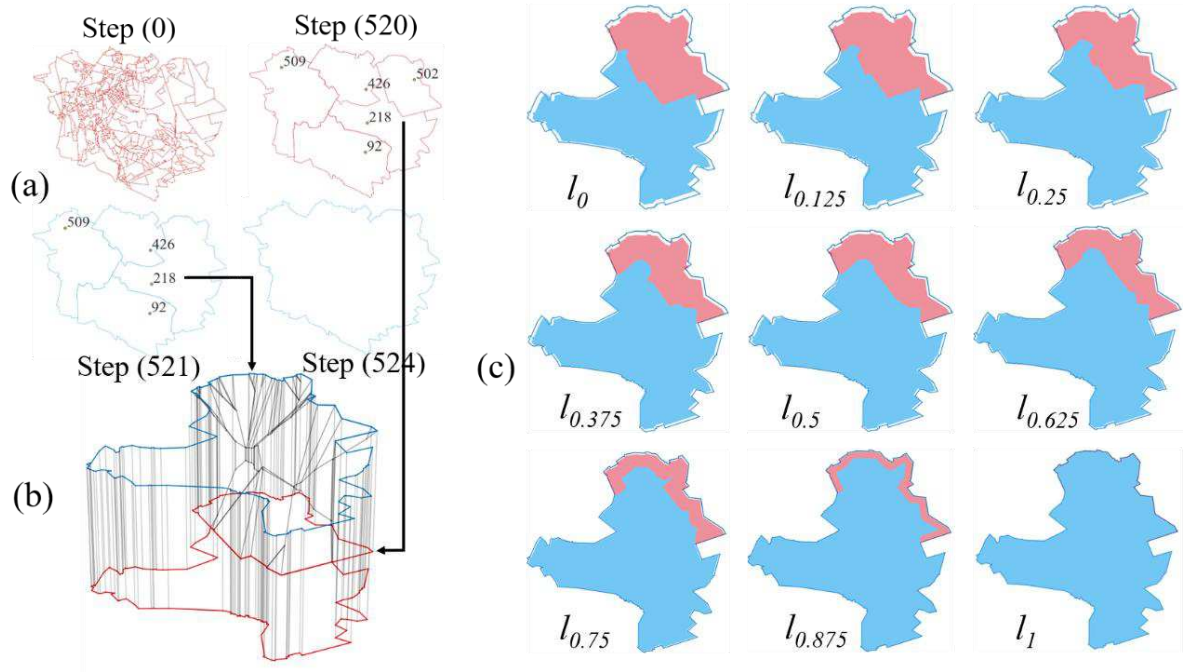


Fig. 10. Application of the first proposed LTS framework to regional hierarchical structures; (a) illustration of the four-step polygonal merging process; (b) constructed LTS for the smooth merging of two neighboring polygonal regions; (c) top-view visualization of horizontal slicing.

The polygon-to-boundary-line construction illustrated in Fig. 10b collapses polygon 502 onto its non-shared boundary line (ID 218). Tracking the number of edges composing the shared boundary across the nine horizontal slices of the resulting LTS reveals a non-monotonic transition, from 12 edges at the source level (l_0) to 49 edges at the target level (l_1) — matching the fixed, topologically invariant edge count of the non-shared boundary line, which remains constant throughout all nine slices. Between these endpoints, the edge count exhibits localized fluctuation (12→10→11→20→19→18→24→36→49) rather than a linear progression. This behavior reflects a shift in which geometric configuration dominates the straight-skeleton bisector structure of the shared boundary: near l_0, the shared boundary is governed primarily by the leaving faces of the source polygon, producing minor edge-collapse events; as the sweep progresses toward l_1, the bisector structure increasingly reflects the meeting faces adjacent to the target line, pulling the edge count toward the target's own vertex density. Because these two governing configurations differ geometrically, the transition is not linear in edge count, even though the underlying area/positional transformation remains smooth and monotonic — mirroring the invariant-reference behavior observed for the parent polygon in the Fig. 11, where the target geometry likewise remains fixed while the transitioning source geometry evolves toward it.

The second strategy performs simultaneous collapse when the target completely encompasses the source geometries. It combines polygon-to-boundary-polyline transitions for source polygons adjacent to the target boundary with polygon-to-point transitions for internal polygons. This approach was applied to the administrative hierarchy of Poland, focusing on the Lower Silesian Voivodeship between LoD2 and LoD1. Since the symmetric difference between the source and target is empty, the combined strategy allows internal county polygons to disappear while boundary polygons progressively transform into the larger voivodeship boundary (Fig. 11b). The resulting LTS provides continuous intermediate representations through slicing (Fig. 11c).

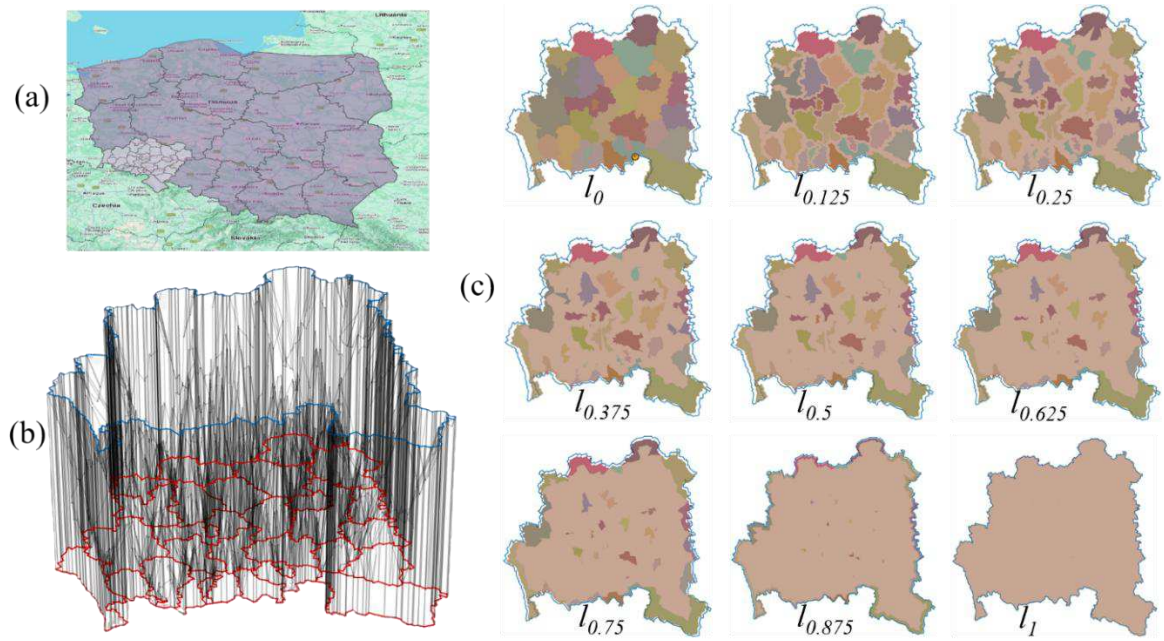


Fig. 11. Application of the second proposed LTS different of regional hierarchical structures; (a) administrative boundaries of Poland—light purple and gray polygons show LoD1 and LoD2; (b) constructed LTS for the administrative boundaries; (c) top-view visualization of horizontal slicing; each source polygon is illustrated with an individual color, and target polygon is shown with light brown.

To quantitatively evaluate this transition, the geometric evolution of the 29 source county polygons was examined across nine horizontal slices. Table 2 summarizes the total edges and faces count, number of features split into multiple faces, and number of features that had completely collapsed at each LoD.

The results in Table 2 show that all 29 source features are ultimately collapsed. The edge and face count does not vary monotonically because the transition geometry is governed by different straight-skeleton configurations near the source and target states. Nevertheless, the overall geometric transformation remains continuous and monotonic. As shown in Table 2, the number of split features increases over the interval $[l_0, l_{0.5}]$ and then decreases monotonically over $[l_{0.5}, l_1]$, whereas the number of collapsed features increases monotonically throughout.

Overall, the experiments demonstrate that the proposed LTS framework can represent both regular and complex real-world transformations. The Great Neck case demonstrates polygonal aggregation, the South Aegean case demonstrates simultaneous heterogeneous generalization operations, and the ATKIS and Lower Silesian cases demonstrate hierarchical transformations where the symmetric difference between source and target is empty. In all

cases, horizontal slicing provides continuous intermediate representations across the LoD range.

Table 2. Aggregate geometric statistics for the 29 source county polygons across the nine horizontal slices of the LTS shown in Fig. 11c.

Slice	Total edges	Total faces	Features that split (>1 face)	Features already collapsed
l_0	2125	30	0	0
$l_{0.125}$	1894	37	6	0
$l_{0.25}$	1612	51	13	0
$l_{0.375}$	1389	51	11	1
$l_{0.5}$	1202	55	16	3
$l_{0.625}$	1035	42	6	4
$l_{0.75}$	966	41	7	4
$l_{0.875}$	877	35	5	14
$l1$	902	1	0	29

5. Discussion

Some transformations represent challenging or "unsatisfying cases," such as when source and target polygons become disjoint after projection or when two polylines cannot directly form a valid LTS. These cases can be handled by first applying appropriate displacement or orientation to establish the required correspondence, constructing the LTS, and then gradually applying the displacement or orientation to the intermediate LoDs. This enables smooth transitions even when standard morphing approaches cannot directly establish a valid transition.

A key advantage of the proposed framework is that the LTS consists of planar faces, reducing geometric complexity while maintaining monotonicity during transformation. Unlike

approaches that triangulate straight-skeleton-based transition surfaces, the proposed method directly extrudes skeletal faces into the LTS. This avoids unnecessary triangulation and reduces the number of faces while providing a suitable structure for dynamic horizontal slicing. The planar representation also supports stable geometric evolution and, when integrated with the DHE structure, provides a topological basis for maintaining feature connectivity during scale transitions.

A specific LoD can be extracted by intersecting the 2D+1D LTS with a horizontal plane at the corresponding LoD value. Although a slice may occasionally produce multiple geometric primitives, these represent parts of a single continuous 3D feature. To maintain semantic and topological consistency in such cases, three mechanisms are employed: (1) attribute propagation, by assigning the original feature attributes to the resulting fragments; (2) structural connectivity, by connecting fragments using bridge edges derived from the straight skeleton; and (3) geometric adjustment, by normalizing skeleton nodes to eliminate valleys and ensure a consistent collapse toward the target representation.

These properties make the proposed LTS suitable for complex continuous LoD transformations while maintaining geometric simplicity, topological consistency, and efficient slicing. Further research is required to systematically evaluate the remaining unsatisfactory configurations and extend the framework to additional transformation scenarios.

6. Conclusion

This paper presented a generalized LoD Transition Space (LTS) framework for constructing smooth and continuous transitions between geometric features within a vario-scale representation environment. Building upon previous work on polygon-to-point transitions based on straight skeletons and dual half-edge structures, this approach extends the concept of continuous LoD modeling to support a broader range of transformations, including polygon-to-polygon, polygon-to-polyline, polyline-to-polyline, and many-to-one polygon transitions.

The proposed framework models geometric transformations as continuous 2D+1D solid volumes, where the additional dimension represents the LoD evolution parameter. By decomposing transformations into localized LoD Transition Regions and constructing dedicated transition primitives for each, the method enables the generation of infinitely many intermediate representations through horizontal slicing while preserving geometric continuity and topological consistency.

The framework supports several important map generalization operations, including merging, aggregation, simplification, splitting, collapsing, and smoothing. Experimental results using synthetic examples and real-world datasets demonstrate that the proposed method effectively handles complex polygonal structures, multipart geometries, and hierarchical regional transformations while maintaining smooth transitions across scales.

The presented approach currently focuses on topological cases in which source and target geometries exhibit overlapping interiors. Non-satisfying relationships, such as disjoint and touching configurations, remain challenging because they require additional mechanisms to preserve spatial continuity during the transition process. Similarly, smooth transformations between non-overlapping holes and disconnected components require further investigation.

Future work will focus on extending the framework to support disjoint topological relationships, improving the handling of complex many-to-many transformations, and developing automated strategies for transition-region decomposition and correspondence matching. Additional research will also investigate the integration of semantic constraints, adaptive weighting schemes, and GPU-based implementations for real-time continuous map generalization and interactive visualization.

Beyond geographic applications, the proposed LTS framework has potential relevance in other domains involving continuous geometric transformation, including morphing animation, medical shape reconstruction, procedural modeling, and topology-aware geometric editing. Consequently, the framework provides a promising foundation for future research on continuous multi-scale geometric representation and topology-preserving spatial transformation.

Declaration of generative AI and AI-assisted technologies in the manuscript preparation process

During the preparation of this work the authors used Jenni AI and ChatGPT (OpenAI) in order to improve the clarity, organization, and language of the manuscript. After using this tool/service, the authors reviewed and edited the content as needed and took full responsibility for the content of the published article.

Funding

This work was supported by the National Science Centre (NCN), Poland under Grant 2021/41/B/ST10/03178.

Notes on contributors

Amin Gholami is a doctoral researcher at the Institute of Geodesy and Geoinformatics, Wroclaw University of Environmental and Life Sciences (UPWr). His research focuses on developing a topological data structure to support multidimension representation.

Pawel Boguslawski is an associate professor at the Institute of Geodesy and Geoinformatics, Wroclaw University of Environmental and Life Sciences (UPWr). He is an expert in topological data structures and the developer of the DHE model. He is the principal investigator who secured funding to support the project, which results are presented in this manuscript.

Martijn Meijers is an assistant professor at the Faculty of Architecture and the Built Environment, Delft University of Technology (TU Delft). He specializes in automated map generalization and multi-scale spatial modeling.

Competing interests

The author(s) declare no competing interests.

Data availability statement

The datasets analyzed in this study are publicly available from their respective data providers. The ATKIS Digital Basic Landscape Model dataset was obtained through the European Data Portal (https://data.europa.eu/data/datasets/d2eaa212-f68d-4e2d-a7e7-8e8063d1b855). The building-footprint data for the Great Neck, New York, case study were obtained from OpenStreetMap (OSM) using the Overpass Turbo API (https://overpass-turbo.eu/). The NUTS 2024 datasets were obtained from the Eurostat GISCO database (https://ec.europa.eu/eurostat/web/gisco/geodata/statistical-units/territorial-units-statistics). The Polish administrative boundaries and BDOT10k datasets were obtained from the Head Office of Geodesy and Cartography (GUGiK) through the national geoportal (https://mapy.geoportal.gov.pl/). Access to and reuse of these datasets are subject to the terms and conditions of their respective data providers. The processed data and LTS representations generated in this study are available from the corresponding author upon reasonable request, subject to the licensing conditions of the original datasets.

Author contributions

A.G. conceived the study, developed the methodology, implemented the software, conducted the investigation and formal analysis, and prepared the visualizations. A.G. wrote the original manuscript. P.B. contributed to the methodology, supervised the research, and reviewed and

edited the manuscript. M.M. contributed to the methodology, supervised the research, and reviewed and edited the manuscript. All authors reviewed and approved the final manuscript.

References

Ai, T., 2010. Constraints of progressive transmission of spatial data on the web. Geo-spatial Information Science 13, 85–92. https://doi.org/10.1007/s11806-010-0219-8

Ai, T., Li, J., 2009. The lifespan model of GIS data representation over scale space, in: 2009 17th International Conference on Geoinformatics. IEEE, pp. 1–6. https://doi.org/10.1109/GEOINFORMATICS.2009.5293369

Aichholzer, O., Aurenhammer, F., Alberts, D., Gärtner, B., 1996. A Novel Type of Skeleton for Polygons, in: Maurer, H., Calude, C., Salomaa, A. (Eds.), J.UCS The Journal of Universal Computer Science. Springer Berlin Heidelberg, Berlin, Heidelberg, pp. 752–761. https://doi.org/10.1007/978-3-642-80350-5_65

Barequet, G., Goodrich, M.T., Levi-Steiner, A., Steiner, D., 2003a. Straight-skeleton based contour interpolation, in: Proceedings of the Fourteenth Annual ACM-SIAM Symposium on Discrete Algorithms. pp. 119–127.

Barequet, G., Vaxman, A., 2007. Nonlinear interpolation between slices, in: Proceedings of the 2007 ACM Symposium on Solid and Physical Modeling. Presented at the SPM07: Symposium on Solid and Physical Modeling, ACM, Beijing China, pp. 97–107. https://doi.org/10.1145/1236246.1236262

Biedl, T., Held, M., Huber, S., Kaaser, D., Palfrader, P., 2015. Weighted straight skeletons in the plane. Computational Geometry 48, 120–133. https://doi.org/10.1016/j.comgeo.2014.08.006

Boguslawski, P., 2011. Modelling and analysing 3D building interiors with the dual half-edge data structure.

Boguslawski, P., Gold, C., 2016. The dual half-edge—A topological primal/dual data structure and construction operators for modelling and manipulating cell complexes. ISPRS International Journal of Geo-Information 5, 19. https://doi.org/10.3390/ijgi5020019

Cheng, M., Sun, Q., Chen, H., Yang, N., Xing, Z., Meng, Y., 2023. Global Topology Concept Neighborhood Graph and Its Application in Topological Similarity Measurement, in: Journal of Physics: Conference Series. IOP Publishing, p. 012017. https://doi.org/10.1088/1742-6596/2449/1/012017

Choi, J., Hwang, C.-S., 2009. Multi-scale Rendering with Geometry Collapse and a Symbol Knowledge Base. The Cartographic Journal 46, 155–163. https://doi.org/10.1179/000870409X459914

Dalstein, B., Ronfard, R., Van De Panne, M., 2015. Vector graphics animation with time-varying topology. ACM Trans. Graph. 34, 1–12. https://doi.org/10.1145/2766913

Egenhofer, M.J., Herring, J., 1990. Categorizing binary topological relations between regions, lines, and points in geographic databases. The 9, 76.

Forsch, A., Kemna, R., Langetepe, E., Haunert, J.-H., 2024. Polyline Morphing for Animated Schematic Maps. J geovis spat anal 8, 37. https://doi.org/10.1007/s41651-024-00198-w

Gedicke, S., Oehrlein, J., Haunert, J.-H., 2021. Aggregating land-use polygons considering line features as separating map elements. Cartography and Geographic Information Science 48, 124–139. https://doi.org/10.1080/15230406.2020.1851613

Gholami, A., P. Boguslawski, and M. Meijers. (In press). "Construction Method for Topological Integration of Multi-scale Datasets Supported by a Primal-Dual Data Structure." Geo-spatial Information Science.

Gholami, A., Boguslawski, P., Meijers, M., 2026. Hierarchical Polygon-to-Point Collapsing for Multi-Scale Representation Based on the Straight Skeleton. ISPRS Annals of the Photogrammetry, Remote Sensing and Spatial Information Sciences 11, 21–28. https://doi.org/10.5194/isprs-annals-XI-4-2026-21-2026

Gholami, A., Boguslawski, P., Meijers, M., van Oosterom, P., 2025. 2D to 1D and 2D to 0D Geometry Generalization Based on the Straight Skeleton by the Dual-Half Edge Structure. The International Archives of the Photogrammetry, Remote Sensing and Spatial Information Sciences 48, 513–519. https://doi.org/10.5194/isprs-archives-XLVIII-G-2025-513-2025

Gorshkov, V.G., Murin, D.M., Yakimova, O.P., 2022. Research of models of topological relations of spatial objects. Modelirovanie i Analiz Informatsionnykh Sistem 29, 154–165. https://doi.org/10.18255/1818-1015-2022-3-154-165

Haunert, J.-H., Sester, M., 2008. Area Collapse and Road Centerlines based on Straight Skeletons. Geoinformatica 12, 169–191. https://doi.org/10.1007/s10707-007-0028-x

Huang, L., Ai, T., Van Oosterom, P., Yan, X., Yang, M., 2017. A matrix-based structure for vario-scale vector representation over a wide range of map scales: The case of river network data. ISPRS International Journal of Geo-Information 6, 218. https://doi.org/10.3390/ijgi6070218

Huber, S., 2011. Computing straight skeletons and motorcycle graphs: theory and practice. Shaker.

Jones, C.B., Bundy, G.L., Ware, M.J., 1995. Map generalization with a triangulated data structure. Cartography and Geographic Information Systems 22, 317–331. https://doi.org/10.1559/152304095782540221

Kada, M., Wichmann, A., Hermes, T., 2015. Smooth transformations between generalized 3D building models for visualization purposes. Cartography and Geographic Information Science 42, 306–314. https://doi.org/10.1080/15230406.2015.1039588

Karim, H., Abdul Rahman, A., Boguslawski, P., Meijers, M., Van Oosterom, P., 2017. The Potential of the 3D Dual Half-Edge (DHE) Data Structure for Integrated 2D-Space and Scale Modelling: A Review, in: Abdul-Rahman, A. (Ed.), Advances in 3D Geoinformation, Lecture Notes in Geoinformation and Cartography. Springer International Publishing, Cham, pp. 477–493. https://doi.org/10.1007/978-3-319-25691-7_27

Kels, S., Dyn, N., 2011. Reconstruction of 3D objects from 2D cross-sections with the 4-point subdivision scheme adapted to sets. Computers & Graphics 35, 741–746. https://doi.org/10.1016/j.cag.2011.03.007

Kronenfeld, B.J., Stanislawski, L.V., Buttenfield, B.P., Brockmeyer, T., 2020. Simplification of polylines by segment collapse: minimizing areal displacement while preserving area. International Journal of Cartography 6, 22–46. https://doi.org/10.1080/23729333.2019.1631535

Li, C., Yin, Y., Wu, P., Liu, X., Guo, P., 2018. Improved jitter elimination and topology correction method for the split line of narrow and long patches. ISPRS International Journal of Geo-Information 7, 402. https://doi.org/10.3390/ijgi7100402

Li, C., Yin, Y., Wu, P., Wu, W., 2022. A partitioned collapse method for long and narrow patches. Computers & Geosciences 159, 104984. https://doi.org/10.1016/j.cageo.2021.104984

Li, C., Yin, Y., Wu, P., Wu, W., 2019. Skeleton line extraction method in areas with dense junctions considering stroke features. ISPRS International Journal of Geo-Information 8, 303. https://doi.org/10.3390/ijgi8070303

Li, S., Li, W., Lin, Z., Yi, S., 2019. Method for 3D city building continuous transformation based on an improved LOD topological data structure. ISPRS International Journal of Geo-Information 8, 504. https://doi.org/10.3390/ijgi8110504

Liu, P., Li, X., Liu, W., Ai, T., 2016. Fourier-based multi-scale representation and progressive transmission of cartographic curves on the internet. Cartography and Geographic Information Science 43, 454–468. https://doi.org/10.1080/15230406.2015.1088799

Meijers, B.M., 2011. Variable-scale Geo-information. NCG Delft.

Meijers, B.M., van Oosterom, P.J.M., 2011. THE SPACE-SCALE CUBE: AN INTEGRATED MODEL FOR 2D POLYGONAL AREAS AND SCALE. The International Archives of the Photogrammetry, Remote Sensing and Spatial Information Sciences XXXVIII-4-C21, 95–102. https://doi.org/10.5194/isprsarchives-XXXVIII-4-C21-95-2011. https://doi.org/10.5194/isprsarchives-XXXVIII-4-C21-95-2011

Oliva, J., Perrin, M., Coquillart, S., 1996. 3D Reconstruction of Complex Polyhedral Shapes from Contours using a Simplified Generalized Voronoi Diagram. Computer Graphics Forum 15, 397–408. https://doi.org/10.1111/1467-8659.1530397

Ren, J., Zhang, B., Wu, B., Huang, J., Fan, L., Ovsjanikov, M., Wonka, P., 2021. Intuitive and Efficient Roof Modeling for Reconstruction and Synthesis. https://doi.org/10.48550/arXiv.2109.07683

Rolland, J., Boutin, R., Eveillard, D., Delahaye, B., 2024. Datascape: exploring heterogeneous dataspace. Scientific Reports 14, 7041. https://doi.org/10.1038/s41598-024-52493-7

Rottmann, P., Driemel, A., Haverkort, H., Röglin, H., Haunert, J.-H., 2025. Bicriteria Shapes: Hierarchical Grouping and Aggregation of Polygons with an Efficient Graph-Cut Approach. ACM Trans. Spatial Algorithms Syst. 11, 1–23. https://doi.org/10.1145/3705001

Rottmann, P., Driemel, A., Haverkort, H., Röglin, H., Haunert, J.-H., 2021. Bicriteria Aggregation of Polygons via Graph Cuts. LIPIcs, Volume 208, GIScience 2021 208, 6:1-6:16. https://doi.org/10.4230/LIPICS.GISCIENCE.2021.II.6

Saalfeld, A., 1999. Topologically Consistent Line Simplification with the Douglas-Peucker Algorithm. Cartography and Geographic Information Science 26, 7–18. https://doi.org/10.1559/152304099782424901

Sarmah, M., Neelima, A., Singh, H.R., 2023. Survey of methods and principles in three-dimensional reconstruction from two-dimensional medical images. Vis. Comput. Ind. Biomed. Art 6, 15. https://doi.org/10.1186/s42492-023-00142-7

Schiavina, M., Melchiorri, M., Freire, S., 2023. A smart and flexible approach for aggregation of adjacent polygons to meet a minimum target area or attribute value. Scientific Reports 13, 4367. https://doi.org/10.1038/s41598-023-31253-z

Strano, E., Nicosia, V., Latora, V., Porta, S., Barthélemy, M., 2012. Elementary processes governing the evolution of road networks. Scientific reports 2, 296. https://doi.org/10.1038/srep00296

Šuba, R., Meijers, M., Oosterom, P. van, 2016. Continuous road network generalization throughout all scales. ISPRS International Journal of Geo-Information 5, 145.

Tinghua, A., Yaolin, L., 2003. Spatial relation resolution and spatial relation abstraction. Geo-spatial Information Science 6, 10–16. https://doi.org/10.1007/BF02826944

Torres-Avilés, R., Santolaya, F., Caniupán, M., Gutiérrez, G., 2025. A Discrete Model for Representing and Computing Topological Relationships Between Polygons, in: 2025 44th International Conference of the Chilean Computer Science Society (SCCC). IEEE, pp. 1–7. https://doi.org/10.1109/SCCC67219.2025.11420703

Turk, G., O'Brien, J.F., 2005. Shape transformation using variational implicit functions, in: ACM SIGGRAPH 2005 Courses on - SIGGRAPH '05. Presented at the ACM SIGGRAPH 2005 Courses, ACM Press, Los Angeles, California, p. 13. https://doi.org/10.1145/1198555.1198639

Van Oosterom, P., 2005. Variable-scale Topological Data Structures Suitable for Progressive Data Transfer: The GAP-face Tree and GAP-edge Forest. Cartography and Geographic Information Science 32, 331–346. https://doi.org/10.1559/152304005775194782

van Oosterom, P., Meijers, M., 2014. Vario-scale data structures supporting smooth zoom and progressive transfer of 2D and 3D data. International Journal of Geographical Information Science 28, 455–478. https://doi.org/10.1080/13658816.2013.809724

Van Oosterom, P., Meijers, M., 2011. Towards a true vario-scale structure supporting smooth-zoom.

Van Oosterom, P., Meijers, M., Stoter, J., Šuba, R., 2014. Data Structures for Continuous Generalisation: tGAP and SSC, in: Burghardt, D., Duchêne, C., Mackaness, W. (Eds.), Abstracting Geographic Information in a Data Rich World, Lecture Notes in Geoinformation and Cartography. Springer International Publishing, Cham, pp. 83–117. https://doi.org/10.1007/978-3-319-00203-3_4

Visvalingam, M., Whyatt, J.D., 2017. Line generalization by repeated elimination of points, in: Landmarks in Mapping. Routledge, pp. 144–155.

Wolf, E.B., 2009. Ontology-Driven Generalization of Cartographic Representations by Aggregation and Dimensional Collapse, in: Bernstein, A., Karger, D.R., Heath, T., Feigenbaum, L., Maynard, D., Motta, E., Thirunarayan, K. (Eds.), The Semantic Web - ISWC 2009, Lecture Notes in Computer Science. Springer Berlin Heidelberg, Berlin, Heidelberg, pp. 990–997. https://doi.org/10.1007/978-3-642-04930-9_65

Yang, X., Huo, L., Shen, T., Wang, X., Yuan, S., Liu, X., 2024. A large-scale urban 3D model organisation method considering spatial distribution of buildings. IET Smart Cities 6, 54–64. https://doi.org/10.1049/smc2.12070

Yang, Z., Cui, H., Yang, F., 2021. A Conceptual Framework for Multi-Scale Representation of Geospatial Vector Data, in: 2021 28th International Conference on Geoinformatics. IEEE, pp. 1–5. https://doi.org/10.1109/IEEECONF54055.2021.9687653

Zeng, S., Geng, G., Gao, H., Zhou, M., 2021. A novel geometry image to accurately represent a surface by preserving mesh topology. Scientific Reports 11, 22573. https://doi.org/10.1038/s41598-021-01722-4

Zhang, X., Touya, G., Meijers, M., 2024. Automated Map Generalization: Emerging Techniques and New Trends (Editorial). J geovis spat anal 8, 11, s41651-024-00174–4. https://doi.org/10.1007/s41651-024-00174-4